SCIENTIFIC REP♦RTS

OPEN

Modern dust aerosol availability in northwestern China

Xunming Wang[1,2], Hong Cheng[3], Huizheng Che[4], Jimin Sun[5], Huayu Lu[6], Mingrui Qiang[7], Ting Hua[8], Bingqi Zhu[1], Hui Li[8], Wenyong Ma[1], Lili Lang[1], Linlin Jiao[1] & Danfeng Li[1]

The sources of modern dust aerosols and their emission magnitudes are fundamental for linking dust with climate and environment. Using field sample data, wind tunnel experiments and statistical analysis, we determined the contributions of wadis, gobi (stony desert), lakebeds, riverbeds, and interdunes to modern dust aerosol availability in the three important potential dust sources including the Tarim Basin, Qaidam Basin, and Ala Shan Plateau of China. The results show that riverbeds are the dominant landscape for modern dust aerosol availabilities in the Qaidam Basin, while wadis, gobi, and interdunes are the main landscapes over the Ala Shan Plateau and Tarim Basin. The Ala Shan Plateau and Tarim Basin are potential dust sources in northwestern China, while the Qaidam Basin is not a major source of the modern dust aerosols nowadays, and it is not acting in a significant way to the Loess Plateau presently. Moreover, most of modern dust aerosol emissions from China originated from aeolian processes with low intensities rather than from major dust events.

Modern dust aerosols generated by aeolian processes[1] play important roles in climate and weather processes[2, 3], provide nutrient and essential elements for terrestrial and marine ecosystems[4–8], become dominant sources of loess[9, 10] and marine sediments[11–13], and thereby contribute significantly to global climate, carbon and biogeo-chemical cycles[14, 15]. On global scale, annual intensities of 0.1–10 μm fraction of dust vary between 981 and 4313 Tg[16], or approximately 1654 Tg yr^{-1} [17] or 1490 Tg yr^{-1} [18], and the 0.1–6 μm fractions range from 1604 to 1960 Tg yr^{-1} [19, 20]. Without considering the contributions of human activities, modern dust aerosols emissions originating from natural sources are 1840 Tg yr^{-1} [21]. These large differences may result in uncertainties in reconstructing and predicting climate and environmental changes of the past and present, determining current air pollution controls, and combating desertification.

In Asia, approximately 400 to 1100 Tg yr^{-1} of modern dust aerosols, or more than 50% of the global total, originate from China such as from the Qaidam Basin, Tarim Basin and Ala Shan Plateau[22–26] (Fig. 1). They are transported over large areas of Asia and across the Pacific to North America[27–30], and the potential landscapes of modern dust aerosol emissions may include gobi[31], sandy deserts[22, 32–35] and other landscapes, such as riverbeds, lakebeds, and wadis (dry ancient lakebed /riverbed that contains water only during the periods of heavy rain or simply an intermittent stream)[36, 37]. However, the heterogeneity of underlying surfaces may result in large differences in aeolian process intensities[38, 39], leading to uncertainties for estimating modern dust aerosol emission quantities and identifying the potential modern dust aerosol source areas in the region.

The amount of fine materials (i.e., <50 μm in diameter) transported by aeolian processes is taken as the dust aerosol availability[40], which is important for understanding the intensity of dust aerosol loading in the region[41]. Although there have been direct measurements of aerosol loadings in Chinese desert regions[22, 42], the absence of direct measurements of modern dust aerosol availabilities in different landscapes gives rise to several uncertainties (S1), especially when 1) simulating global and regional modern dust aerosol emission intensities; 2) assessing the

[1]Key Laboratory of Water Cycle and Related Land Surface Processes, Institute of Geographic Sciences and Natural Resources Research, Chinese Academy of Sciences, Beijing, 100101, China. [2]University of Chinese Academy of Sciences, Beijing, 100049, China. [3]State Key Laboratory of Earth Surface Processes and Resource Ecology, Beijing Normal University, Beijing, 100875, China. [4]State Key Laboratory of Severe Weather (LASW), Institute of Atmospheric Composition, Chinese Academy of Meteorological Sciences, Beijing, 100081, China. [5]Key Laboratory of Cenozoic Geology and Environment, Institute of Geology and Geophysics, Chinese Academy of Sciences, Beijing, 100029, China. [6]School of Oceanographic and Geographic Sciences, Nanjing University, Nanjing, 210023, China. [7]Key Laboratory of Western China's Environmental Systems (Ministry of Education), College of Earth and Environmental Sciences, Lanzhou University, Lanzhou, 730000, China. [8]Key Laboratory of Desert and Desertification, Cold and Arid Regions Environmental and Engineering Research Institute, Chinese Academy of Sciences, Lanzhou, 730000, China. Correspondence and requests for materials should be addressed to X.W. (email: xunming@igsnrr.ac.cn)
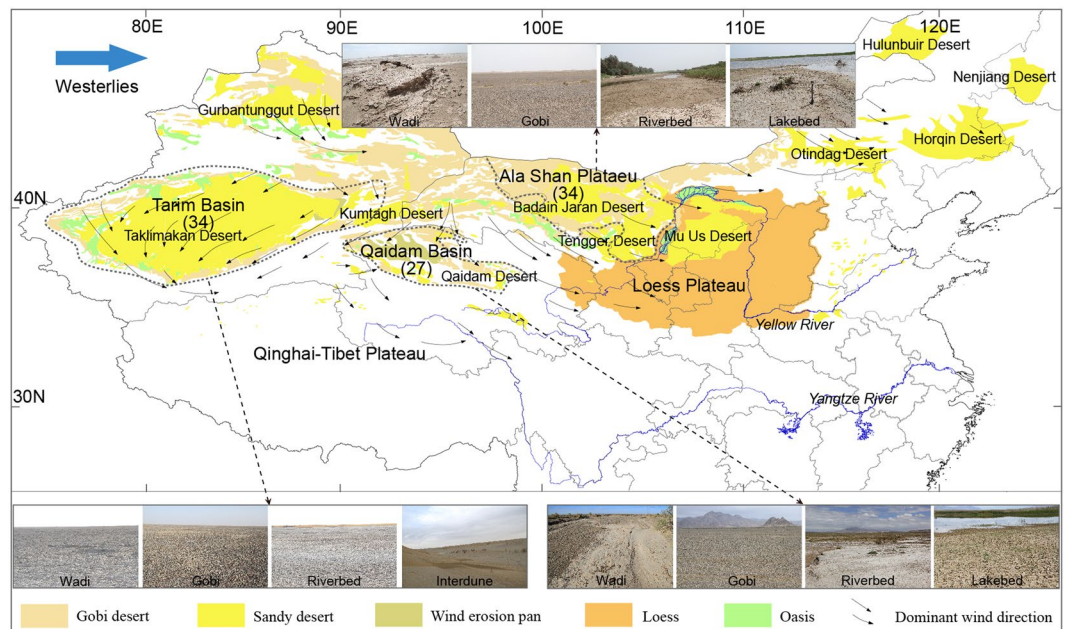
Figure 1. Locations of the Qaidam Basin, Ala Shan Plateau, Tarim Basin, and the landscapes with high modern dust aerosol emissions. Numbers within the brackets are the number of samples. The figure was finished using Arcgis software (version 10.1, ESRI Inc., Redlands, California, USA), which can be downloaded from the internal network of Institute of Geographic Sciences and Natural Resources Research, Chinese Academy of Sciences.
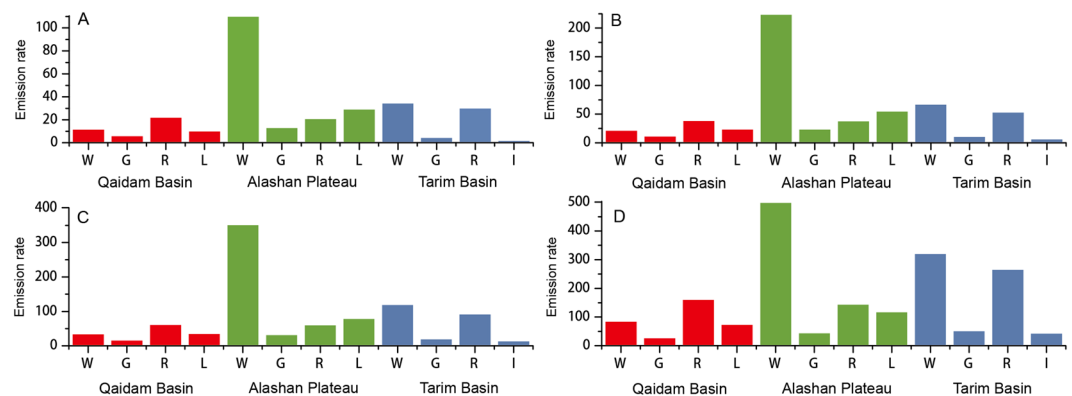

Figure 2. Availabilities of PM2.5 (**A**), PM5 (**B**), PM10 (**C**), and PM50 (**D**) (g m^{-2}) during one aeolian event for different landscapes. W: wadi; G: gobi; R: riverbed; L: lakebed; and I: interdune.

impacts of modern dust aerosols on global climate, carbon and biogeochemical cycles; 3) identifying the source of aeolian sediments that have been employed as proxies in climate reconstructions in the sediment areas[43, 44]. To address this gap, we use field investigations, sampling, wind tunnel experiments, and particle size measurements as well as the statistical analysis to determine modern dust aerosol availabilities of different landscapes over the Tarim Basin, Qaidam Basin and Ala Shan Plateau. The results improve our understanding of modern dust aerosol availabilities and aeolian sediment sources in China.

Results and Discussion

The Qaidam Basin is a potential source of the Loess Plateau during Pleistocene[45]. Landscapes with higher modern dust aerosol availabilities in the Qaidam Basin include riverbeds, wadis and lakebeds (Fig. 2). In the Ala Shan Plateau and Tarim Basin, wadis have relatively higher modern dust aerosol availabilities than other landscapes. Due to extremely low contents of fine fractions (i.e., fractions <50 μm in diameter) in mobile sands, there are nearly no or extremely low fine fractions (i.e., <50 μm in diameter) in the transported materials obtained using collection sampler (*S2*), which indicates that the mobile sand dunes are not the dominant landscape for modern dust aerosol availability. However, in the other regions such as Sahara Desert and western Queensland, aeolian
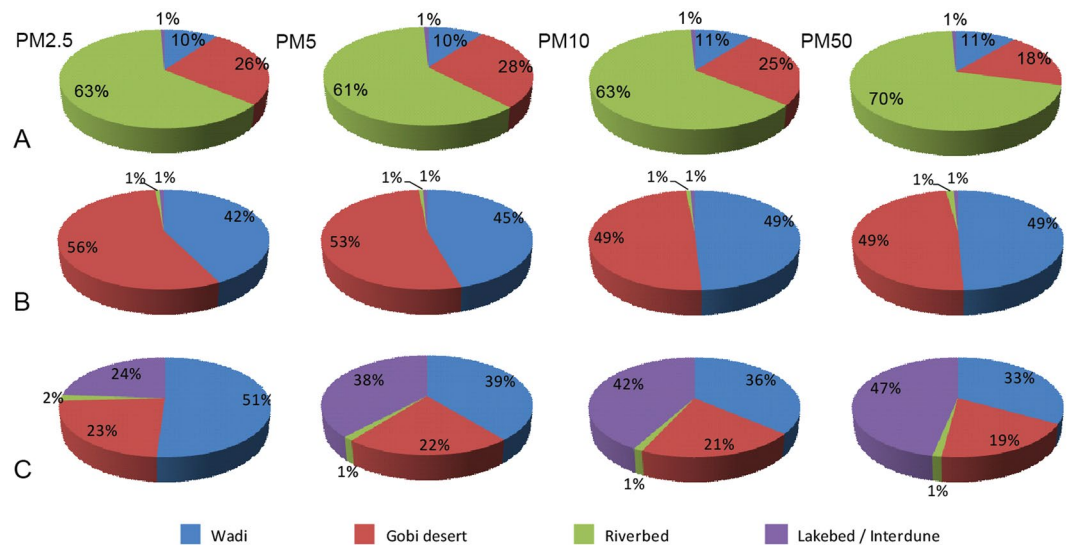
2

Figure 3. The comparison in the availabilities of PM2.5, PM5, PM10 and PM50 among different landscapes. (**A**) Qaidam Basin; (**B**) Ala Shan Plateau; and (**C**) Tarim Basin.

Region	PM2.5	PM5	PM10	PM50
Qaidam Basin	0.663	1.188	1.827	4.383
Alashan Plateau	2.723	5.177	7.545	10.647
Tarim Basin	1.337	3.407	6.533	19.301

Table 1. Availabilities of PM2.5, PM5, PM10 and PM50 (Tg) generated in one heavy dust event in the Qaidam Basin, Ala Shan Plateau and Tarim Basin.

abrasion among sand grains breaks the clay coatings on grain surfaces of the dune sands, which act as the main source of particulate matter less than 10 microns (PM10)[46, 47].

Except for the differences in the dust availability under the same landscape, there are variations in the dust aerosol availability among different landscapes (*S2*). After combining the areas of different landscapes, the results show that more than 60% of PM2.5 to PM50 fractions in the Qaidam Basin is emitted from riverbeds, while the gobi provides only 18–28% in the region (Fig. 3). In sharp contrast to the Qaidam Basin, only 1% of the dust originated from riverbeds in the Ala Shan and Tarim Basin, while the gobi and wadi provide 49–53% and 42–49% of the modern dust aerosol availabilities, respectively. In the Tarim Basin, more than 50% of the PM2.5 fractions are from wadis, while nearly half of the PM50 fractions are emitted from the interdunes located within the mobile sandy deserts.

Without considering the impacts of other regions of China, approximately 58% of the PM2.5 fractions may be generated on the Ala Shan Plateau and approximately 56% of the PM50 fractions may be generated on the Tarim Basin during a single high-intensity aeolian event in China (Table 1). Although the Qaidam Basin was proposed as the dominant dust source during the Quaternary Period for the Loess Plateau[45, 48], the Qaidam Basin is unlikely to be a potential aeolian source for modern dust aerosols and loess sediment in East Asia because the percentages of PM2.5, PM5, PM10 and PM50 availabilities in the Qaidam Basin only occupied 14.04%, 12.16%, 11.49% and 12.77% in the three regions.

Variation in modern dust aerosol availabilities for different landscapes may result in different modern dust aerosol emission responses to climate/environmental changes. In the Qadaim Basin, increases in precipitation, melted snow and glacial meltwater may promote sediment transport to riverbeds and consequently improve modern dust aerosol availabilities in the region. This suggests that global warming on the Qinghai-Tibet Plateau[49, 50] may enhance modern dust aerosol availabilities. In contrast, for the Tarim Basin and Ala Shan Plateau, although environmental deterioration has resulted in most rivers and lakebeds drying up over the past few decades, there has been no significant change in the areas covered by wadis[51], mobile sandy deserts and gobi compared with those during the Quaternary Period[52]. Hence, global warming may not trigger a large increase in erodible fine particles at the surface in these areas and consequently may not increase the modern dust aerosol availabilities in the above two regions. However, global warming may enhance the processes of physical, chemical and salt weathering[38, 53–56] that occur on the surfaces of the gobi, wadis, riverbeds and lakebeds, which would increase modern dust aerosol availabilities.

Finally, more than 80% of modern dust aerosol availabilities in China are from the Ala Shan Plateau, Tarim Basin, and Qaidam Basin[23, 57–59]. According to meteorological records, there have been 2 to 5 annual dust storm events for the three regions from the early 21st century to the present (*S3*). The annual modern dust aerosol availabilities calculated from dust storm events over the three regions for PM2.5, PM5, PM10 and PM50 are

Area (km^2)	Qaidam Basin	Ala Shan Plateau	Tarim Basin
Total	121,000[73]	270,000[74]	530,000[51]
Wadi	5850[75]	10581.3[76]	20,000[77]
Gobi	31,000[78]	120,000[78]	73,000[78]
Riverbed	19,200[79]	1025.14[80]	856.98[81–83]
Lakebed	460[75]	755.92[84]	/
Interdune	/	/	216,000[85]

Table 2. Areas of the Qaidam Basin, Ala Shan Plateau, and Tarim Basin and areas of landscapes with potential modern dust aerosol emission in the region. Note: "/": At present there are only a few lakebeds and interdunes developed in the Tarim Basin, Qaidam Basin and Ala Shan Plateau. Therefore, their areas are negligible.

approximately 18, 36, 56, and 105 Tg, respectively *(S3)*. Therefore, assuming that the magnitude of modern dust aerosol emissions is not overestimated by current dust emission models, the modern dust aerosol emissions in China are related to low-intensity aeolian processes that are below the minimum criteria of the WMO for classification as dust storm events.

Conclusions

Although wadis, gobi, lakebeds, riverbeds, and interdunes are potential landscapes for modern dust aerosol emissions over the Tarim Basin, Qaidam Basin, and the Ala Shan Plateau, their roles in modern dust aerosol availabilities are different. In the Qaidam Basin, riverbeds play a major role in modern dust aerosol availabilities, while for the Ala Shan Plateau and Tarim Basin, wadis, gobi, and interdunes are the dominant landscapes for modern dust aerosol availability. In addition, the Qaidam Basin is not a major potential source of dust for sediment in the Loess Plateau and for modern dust aerosols transported to East Asia and North Pacific regions, at least in the context of modern aeolian processes.

Methodology

Study area. The sampling areas include the Tarim Basin, Ala Shan Plateau and Qaidam Basin with an area of 5,300,000, 2,700,000, and 121,000 km^2, respectively, and are potential sources of modern dust aerosol emission in northwestern China (Fig. 1, Table 2). In these regions, the gobi, which is described as a "wide, shallow basin of which the smooth rocky bottom is filled with sand, silt or clay, pebbles or, more often, with gravel"[60, 61], is extensively developed. In addition to the various landscapes, such as wadi (dry ancient lakebed /riverbed that contains water only during the periods of heavy rain or simply an intermittent stream), the gobi and interdune[37, 39] that have high modern dust aerosol emissions, most water systems in these regions are temporarily developed, causing the riverbeds and lakebeds to dry up, providing abundant fine particles for emission via aeolian processes[38].

Field sampling. Only loose and fine particles on the surface (i.e., <2000 μm in diameter) can be transported by aeolian processes[62] to provide sources for modern dust aerosol emission. In China, these loose and fine particles are typically generated via water erosion, aeolian abrasion and weathering[38, 54–56] and loosely accumulate on land surfaces such as wadis, gobi, lakebeds, interdunes and riverbeds[39]. Because only surface materials with approximately 1–10 cm depth are affected by aeolian processes[63, 64], we collected samples within 10 cm of the surface during field sampling in 2013 and 2014. For each landscape, five representative samples were collected, except for the gobi on the Ala Shan Plateau where 15 samples were collected. In total, ninety-five samples were employed for further wind tunnel experiments. The sampling criteria were as follows: geomorphologic characteristics of the sampling sites are typical landscapes within an area of 10 × 10 km^2, the underlying surfaces have no vegetation cover, no biological or physical soil crusts are present, and no human disturbance is detected. At each site, the samples were collected in horizontal intervals of approximately 100 to 200 m. The particle size characteristic of each landscape is shown in Table 3.

Wind tunnel experiments. Wind tunnel experiments were performed at the Key Laboratory of Desert and Desertification in the Cold and Arid Regions Environmental and Engineering Research Institute, Chinese Academy of Sciences, China. The size and operating characteristics of the wind tunnel were described in detail in previous papers[65–68], and the wind tunnel set-up is shown in Fig. 4.

Before the wind tunnel experiments, all samples were fully crushed and disaggregated. Each sample was spread over an area of 150 × 30 cm in the working section of the wind tunnel, with the surface at the same level as the bottom of the wind tunnel. At a distance of 30 cm downwind from the sample, a trap with 30 cm width and 30 cm height was used to collect windblown material.

According to the observational data from the weather stations in the study area from 1980 to 2014, the maximum wind velocity ranged from 14 to 22 m·s^{-1}. Wind events with velocities of 5–10 m·s^{-1} occupied about 89–100% of those with velocities higher than the threshold wind velocity (5 m·s^{-1}). During our preliminary experiments in November 2009, we found that, no erodible particles existed on the sample surfaces after approximately 360 seconds under a wind velocity of 8 m·s^{-1}, and under a wind velocity of 22 m s^{-1}, no erodible particles existed after 60 seconds. Hence, the free-stream wind velocity at the axis of the wind tunnel were set to 8, 10, 12, 14, 16, 18, 20, and 22 m·s^{-1}. For each free-stream wind velocity, we simultaneously measured the wind velocity at 10 different heights (0.3, 0.6, 1.2, 2.4, 4.0, 8.0, 12.0, 16.0, 20.0, and 25.0 cm) above the floor of the wind tunnel using a wind profile sampler (Fig. 4).

Region	Particle size (μm)	<2.5	<5	<10	<50	<100	<200	<2000
Qaidam Basin	Wadi	4.95	9.04	15.36	52.43	80.75	96.56	100
	Gobi	2.58	4.42	6.24	12.19	26.10	56.90	100
	Riverbed	6.43	10.92	16.47	54.15	81.14	95.26	100
	Lakebed	1.53	2.95	4.39	9.56	17.72	59.49	100
	*Mobile sand	0.00	0.00	0.00	0.00	5.68	58.12	100
Tarim Basin	Wadi	3.93	7.47	17.54	70.22	91.04	99.57	100
	Gobi	2.35	4.47	7.62	19.85	33.18	50.19	100
	Riverbed	5.77	9.77	16.36	47.64	84.87	100.00	100
	Interdune	5.63	9.55	14.91	39.05	71.95	95.05	100
	*Mobile sand	0.00	0.00	0.00	0.00	9.01	57.42	100
Ala Shan Plateau	Wadi	11.06	21.56	40.30	92.41	95.99	97.31	100
	Gobi	4.10	6.81	9.28	14.02	26.47	55.18	100
	Riverbed	8.82	15.32	23.89	62.84	86.91	95.58	100
	Lakebed	3.87	7.24	10.54	17.36	29.95	60.57	100
	*Mobile sand	0.00	0.00	0.00	0.49	3.87	14.54	100

Table 3. Content as a percentage (%) of total particle size for the surface samples collected. *Mobile sand samples for the wind tunnel experiments were collected from the crest or stoss slope of shifting sand dunes.
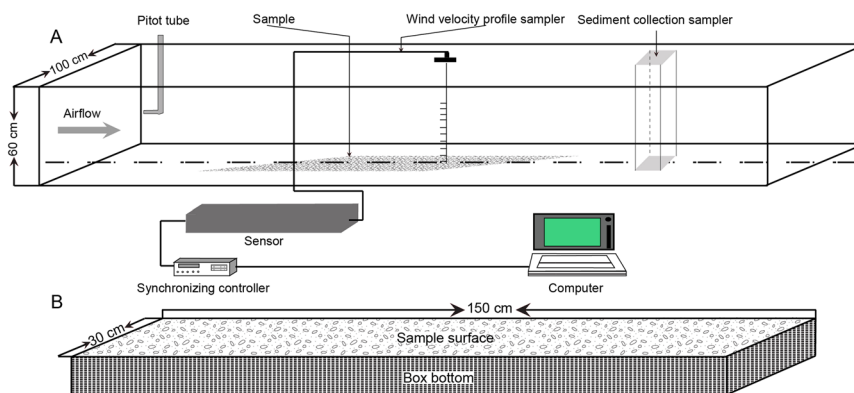

Figure 4. Schematic diagram of (**A**) the wind tunnel and sample arrangement during the wind tunnel experiment, and (**B**) the surface samples.

We started the experiments with a free-stream wind velocity of $8\,m\,s^{-1}$ until all erodible particles in the surface samples were completely eroded. Then, we repeated the experiments until the wind velocity reached $22\,m\cdot s^{-1}$. After all erodible particles in the surface samples were eroded at each wind velocity, the transported sediments collected by the sand trap were weighed and used for particle size analysis. Due to differences in atmospheric circulation[69, 70], vegetation coverage[71], precipitation, topography[39], and subsequent transportation and sediment processes[72], there may be variations in the magnitude of modern dust aerosol availability. Therefore, we discuss only the modern dust aerosol availability in a flat loose bed.

Particle size analysis. After wind tunnel experiments have been finished, the transported and surface materials collected in the field were analyzed for particle size using a Mastersizer 2000 (Malvern Co. Ltd., Malvern, UK). Before conducting the particle size measurements, we immersed the sediments in 10% H_2O_2 followed by immersion in 12.7% HCl to remove any plant debris and disperse aggregates within the sediments. The sample residue was finally treated with 10 mL of 0.05 M $(NaPO_3)_6$ on an ultrasonic vibrator for 10 min to facilitate dispersion before measuring the particle size.

Data processing. During the wind tunnel experiments with increasing wind velocities, the erodible particles were gradually depleted. Therefore, the raw data acquired during the wind tunnel experiments and during the measuring procedures must be re-processed using statistical methods. Stronger winds transport not only coarse materials but also materials that would be transported at lower velocities. Therefore, we used the weighted average method to determine the transports at the certain wind speed:

$$R_w = (R_1M_1 + R_2M_2 + \cdots + R_iM_i + \cdots + R_mM_m)/(M_1 + M_2 + \cdots + M_i + \cdots + M_m) \tag{1}$$

where R_w is the weighted mean of different particle sizes, R_i is the raw data for the contents (%) of different particle sizes at predefined wind velocities (8 to $22\,m\cdot s^{-1}$), and M_i is the corresponding contents of the raw transported

material at the same velocities. Combining the results of particle size analysis, the availabilities of PM2.5, PM5.0, PM10 and PM50 were acquired.

In natural conditions, the bonding abilities of particles, the cover of coarse fractions on the fine particles, and the differences in airflow structures[1], may result in lower contents of loose and fine particles on intact surfaces than on disturbed samples. Therefore, the modern dust aerosol availabilities from the wind tunnel experiments may be higher than those in the field. In addition, meteorological records indicate that the wind velocity rarely exceeds 22 m s⁻¹ during severe dust events. Therefore, we took the transport acquired at a velocity of 22 m·s⁻¹ as the maximum modern dust aerosol availability in the study regions. Additional explanations and discussions are provided in *S2*.

References

1. Shao, Y. *Physics and Modelling of Wind Erosion*. (eds Mysak, L. A. & Hamilton, K.) (Springer, 2008).
2. Bryant, R. G., Bigg, G. R., Mahowald, N. M., Eckardt, F. D. & Ross, S. G. Dust aerosol emission response to climate in southern Africa. *J. Geophys. Res.* **112**, D09207, doi:10.1029/2005JD007025 (2007).
3. IPCC (Intergovernmental Panel on Climate Change). *The Physical Science Basis. Contribution of Working Group I to the Fourth Assessment Report of the Intergovernmental Panel on Climate Change*. (eds Solomon, S. *et al.*) (Cambridge University Press, 2007).
4. Reynolds, R., Belnap, J., Reheis, M., Lamothe, P. & Luiszer, F. Aeolian dust in Colorado Plateau soils: nutrient inputs and recent change in source. *Proc. Natl. Acad. Sci.* **98**, 7123–7127 (2001).
5. Bishop, J. K. B., Davis, R. E. & Sherman, J. T. Robotic observations of dust storm enhancement of carbon biomass in the North Pacific. *Science* **298**, 817–821 (2002).
6. Tsuda, A. *et al.* mesoscale iron enrichment in the western Subarctic Pacific induces a large centric diatom bloom. *Science* **300**, 958–961 (2003).
7. Boy, J. & Wilcke, W. Tropical Andean forest derives calcium and magnesium from Saharan dust. Global Biogeochem. *Cy.* **22**, GB1027, doi:10.1029/2007GB002960 (2008).
8. Evan, A., Flamant, C., Gaetani, M. & Guichard, F. The past, present and future of African dust. *Nature* **531**, 493–495 (2016).
9. Liu, T. Loess and Environments. *J. Xi'an Jiaotong University (Social Sciences)* **22**(4), 7–12, doi:10.3969/j.issn.1008-245X.2002.04.002 (2002).
10. Maher, B. A., Mutch, T. J. & Cunningham, D. Implications for provenance of the Chinese Loess Plateau. Magnetic and geochemical characteristics of Gobi Desert surface sediments. *Geology* **37**, 279–282 (2009).
11. Duce, R. A., Unni, C. K., Ray, B. J., Prospero, J. M. & Merrill, J. T. Long-range atmospheric transport of soil dust from Asia to the Tropical North Pacific: temporal variability. *Science* **209**, 1522–1524 (1980).
12. Duce, R. A. & Tindale, N. W. Chemistry and biology of iron and other trace metals. *Limnology Oceanography* **36**, 1715–1726 (1991).
13. Leinen, M., Prospero, J. M., Arnold, E. & Blan, M. Mineralogy of aeolian dust reaching the North Pacific Ocean, 1, Sampling and analysis. *J. Geophys. Res.* **99**, 21017–21023 (1994).
14. Petit, J. R. *et al.* Climate and atmospheric history of the past 420,000 years from the Vostok ice core, Antarctica. *Nature* **399**, 429–436 (1999).
15. Jickells, T. D. *et al.* Global iron connections between desert dust, ocean biogeochemistry, and climate. *Science* **308**, 67–71 (2005).
16. Huneeus, N. *et al.* Global dust model intercomparison in AeroCom phase I. *Atmos. Chem. Physics* **11**(15), 7781–7816 (2011).
17. Luo, C., Mahowald, N. & Corral, J. Sensitivity study of meteorological parameters on mineral aerosol mobilization, transport, and distribution. *J. Geophys. Res.* **108**(D15), 4447, doi:10.1029/2003JD003483 (2003).
18. Griggs, D. J. & Noguer, M. Climate Change 2001: The scientific basis. Contribution of Working Group I to the Third Assessment Report of the Intergovernmental Panel on Climate Change. *Weather* **57**(8), 267–269 (2002).
19. Ginoux, P., Prospero, J., Gill, T., Hsu, N. & Zhao, M. Global-scale attribution of anthropogenic and natural dust sources and their emission rates based on MODIS Deep Blue aerosol products. *Rev. Geophys.* **50**, RG3005, doi:10.1029/2012RG000388 (2012).
20. Ginoux, P. *et al.* Sources and distributions of dust aerosols simulated with the GOCART model. *J. Geophys. Res.* **106**(D17), 20255–20273 (2001).
21. Tegen, I., Werner, M., Harrison, S. & Kohfeld, K. Relative importance of climate and land use in determining present and future global soil dust aerosol emission. *Geophys. Res. Lett.* **31**, L05105, doi:10.1029/2003GL019216 (2004).
22. Zhang, X., Arimoto, R. & An, Z. Dust emission from Chinese desert sources linked to variations in atmospheric circulation. *J. Geophys. Res.* **102**(D23), 28041–28047 (1997).
23. Zhang, X. *et al.* Sources of Asian dust and role of climate change versus desertification in Asian dust aerosol emission. *Geophys. Res. Lett.* **30**(24), 2272, doi:10.1029/2003GL018206 (2003).
24. Zender, C., Bian, H. & Newman, D. Mineral Dust Entrainment and Deposition (DEAD) model: Description and 1990s dust climatology. *J. Geophys. Res.* **108**(D14), 4416, doi:10.1029/2002JD002775 (2003).
25. Gong, S. *et al.* Characterization of soil dust aerosol in China and its transport and distribution during 2001 ACE-Asia: 2. Model simulation and validation. *J. Geophys. Res.* **108**(D9), 4262 (2003).
26. Liu, C. *et al.* Observational study of formation mechanism, vertical structure, and dust aerosol emission of dust devils over the Taklimakan Desert, China. *J. Geophys. Res.* **121**(7), 3608–3618 (2016).
27. Husar, R. B. *et al.* Asian dust events of April 1998. *J. Geophys. Res.* **106**(D16), 18317–18330 (2001).
28. Prospero, J. M., Ginoux, P., Torres, O., Nicholson, S. E. & Gill, T. E. Environmental characterization of global sources of atmospheric soil dust identified with the Nimbus 7 total ozone mapping spectrometer (TOMS) absorbing aerosol product. *Rev. Geophys.* **40**(1), 2-1–2-31 (2002).
29. Sassen, K. Indirect climate forcing over the western US from Asian dust storms. *Geophys. Res. Lett.* **29**(10), 103-1–103-4 (2002).
30. Sun, J., Zhang, M. & Liu, T. Spatial and temporal characteristics of dust storms in China and its surrounding regions, 1960–1999. *J Geophys. Res.* **106**(D10), 10325–10333 (2001).
31. Sun, J., Liu, T. & Lei, Z. Sources of heavy dust fall in Beijing, China on April 16, 1998. *Geophys. Res. Lett.* **27**, 2105–2108 (2000).
32. Bory, A. J. M., Biscaye, P. E., Svensson, A. & Grousset, F. E. Seasonal variability in the origin of recent atmospheric mineral dust at NorthGRIP Greenland. *Earth Planet. Sci. Lett.* **196**, 123–134 (2002).
33. Xuan, J. & Sokolik, N. Characterization of sources and emission rates of mineral dust in Northern China. *Atmos. Environ.* **36**, 4863–4876 (2002).
34. Zhang, B., Tsunekawa, A. & Tsubo, M. Contributions of sandy lands and stony deserts to long-distance dust aerosol emission in China and Mongolia during 2000–2006. *Global Planet. Change* **60**, 487–504 (2008).
35. Cheng, T., Lu, D., Wang, C. & Xu, Y. Chemical characteristics of Asian dust aerosol from Hunshan Dake Sandland in northern China. *Atmos. Environ.* **39**, 2903–2911 (2005).
36. Derbyshire, E., Meng, X. & Kemp, R. A. Provenance, transport and characteristics of modern Aeolian dust in western Gansu Province, China, and interpretation of Quaternary loess record. *J. Arid Environ.* **39**, 497–516 (1998).
37. Wang, X., Dong, Z., Yan, P., Yang, Z. & Hu, Z. Surface sample collection and dust source analysis in northwestern China. *Catena* **59**, 35–53 (2005).

38. Wang, X., Xia, D., Wang, T., Xie, X. & Li, J. Dust sources in arid and semiarid China and southern Mongolia: impacts of geomorphologic setting and surface materials. *Geomorphology* **97**, 583–600 (2008).
39. Wang, X., Zhou, Z. & Dong, Z. Control of dust aerosol emissions by geomorphic conditions, wind environments and land use in northern China: An examination based on dust storm frequency from 1960 to 2003. *Geomorphology* **29**, 292–308 (2006).
40. Kocurek, G. & Lancaster, N. Aeolian system sediment state: theory and Mojave Desert Kelso dune field example. *Sedimentology* **46**, 505–515 (1999).
41. Gerson, R., Amit, R. & Grossman, S. Dust Availability in Desert Terrains. DAJA-83-C-0041, US Army Research, Development and Standardization Group, UK, The Institute of Earth Sciences, The Hebrew University, Jerusalem, 111pp (1985).
42. Zhang, X., Arimoto, R., Zhu, G., Chen, T. & Zhang, G. Concentration, size-distribution and deposition of mineral aerosol over Chinese desert regions. *Tellu.s* **50B**, 317–330 (1998).
43. Hao, Q. & Guo, Z. Spatial variations of magnetic susceptibility of Chinese loess for the last 600 kyr: implications for monsoon evolution. *J. Geophys. Res.* **110**, B12101 (2005).
44. Bory, A. J. M., Biscaye, P. E. & Grousset, F. E. Two distinct seasonal Asian source regions for mineral dust deposited in Greenland (NorthGRIP). *Geophys. Res. Lett.* **30**, 1167 (2003).
45. Pullen, A. *et al.* Qaidam Basin and northern Tibetan Plateau as dust sources for the Chinese Loess Plateau and paleoclimatic implications. *Geology* **39**, 1031–1034 (2011).
46. Bullard, J. E. & White, K. H. Dust production and the release of iron oxides resulting from the aeolian abrasion of natural dune sands. *Earth Surf. Proc. Land.* **30**, 95–106 (2005).
47. Crouvi, O., Schepanski, K., Amit, R., Gillespie, A. R. & Enzel, Y. Multiple dust sources in the Sahara Desert: The importance of sand dunes. *Geophys. Res. Let.* **39**, L13401 (2012).
48. Stevens, T., Palk, C., Carter, A., Lu, H. & Clift, P. D. Assessing the provenance of loess and desert sediments in northern China using U-Pb dating and morphology of detrital zircons. *Geol. Soc. Amer. Bull.* **122**, 1331–1344 (2010).
49. Kato, T. *et al*. Temperature and biomass influences on interannual changes in CO2 exchange in an alpine meadow on the Qinghai–Tibetan Plateau. *Global Change Biol.* **12**, 1285–1298 (2006).
50. Immerzeel, W. W., van Beek, L. P. H. & Bierkens, M. Climate change will affect the Asian water towers. *Science* **328**, 1382–1387 (2010).
51. Song, Y., Wang, R. & Peng, Y. Water resources and ecological conditions in the Tarim Basin. *Sci. China Earth Sci.* **45**, 11–17 (2002).
52. Sun, J. & Liu, T. The age of the Taklimakan Desert. *Science* **312**, 1621 (2006).
53. McFadden, L. D., Eppes, M. C., Gillespie, A. R. & Hallet, B. Physical weathering in arid landscapes due to diurnal variation in the direction of solar heating. *Geol. Soc. Am. Bull.* **117**, 161–173 (2005).
54. Cooke, R. U. & Smalley, I. J. Salt weathering in deserts. *Nature* **220**, 1226–1227 (1968).
55. Wright, J. Making loess-sized silt: data from laboratory simulations and implications for sediment transport pathways and the formation of 'desert' loess deposits associated with the Sahara. *Quat. Int.* **76–77**, 7–19 (2001).
56. Wright, J., Smith, B. & Whalley, B. Mechanisms of loess-sized quartz silt production and their relative effectiveness: laboratory simulations. *Geomorphology* **23**, 15–34 (1998).
57. Sun, J. Source regions and formation of the Loess sediments on the high mountain regions of northwestern China. *Quat. Res.* **58**(3), 341–351 (2002).
58. Hülle, D. *et al*. OSL dating of sediments from the Gobi Desert, Southern Mongolia. *Quat. Geochronol.* **5**, 107–113 (2010).
59. Han, Y. *et al*. The contribution of dust devils and dusty plumes to the aerosol budget in western China. *Atmos. Environ.* **126**, 21–27 (2016).
60. Cable, M. and French, F. *The Gobi Desert*. (eds Hodder & Stoughton) **4**(22) 133-b-135 (Oxford University Press, 1943).
61. Cooke, R. U. Stone pavement in deserts. *Ann. Assoc. Am. Geogr.* **60**, 560–577 (1970).
62. Bagnold, R. A. The Physics of Blown Sand and Desert Dunes. *Nature* **18**(4), 167–187 (1974).
63. Cornelis, W. M. *Dryland Ecohydrology* (eds D'Odorico, P. & Porporato, A) Ch. 9, *Hydroclimatology of wind erosion in arid and semi-arid environments.* 141–159 (Springer, 2006).
64. Zheng, X. & Huang, N. *Mechanics of wind-blown sand movements* (eds Allan, R., Förstner, U. & Salomons, W.) Environmental Science and Engineering Subseries: Environmental Science (Springer, 2009).
65. Dong, Z., Wang, H., Liu, X. & Wang, X. The blown sand flux over a sandy surface: a wind tunnel investigation on the fetch effect. *Geomorphology* **57**, 117–127 (2004).
66. Wang, X. *et al.* Characteristics of the Gobi desert and their significance for dust aerosol emissions in the Ala Shan Plateau (Central Asia): an experimental study. *J. Arid Environ.* **81**, 35–46 (2012).
67. Wang, X., Lang, L., Zhang, C., Hua, T. & Wang, H. The influence of near-surface winds on Sr isotope composition of aeolian sediments: a wind tunnel experiment. *Chemical Geol.* **308–309**, 10–17 (2012).
68. Wang, X., Lang, L., Hua, T., Zhang, C. & Xia, D. Geochemical and magnetic characteristics of aeolian transported materials under different near-surface wind fields: an experimental study. *Geomorphology* **239**, 106–113 (2015).
69. Fan, K. & Wang, H. Antarctic oscillation and the dust weather frequency in North China. *Geophys. Res. Lett.* **31**, L10201 (2004).
70. Ding, R., Li, J., Wang, S. & Ren, F. Decadal change of the spring dust storm in northwest China and the associated atmospheric circulation. *Geophys. Res. Lett.* **32**, L202808 (2005).
71. Zou, X. & Zhai, P. Relationship between vegetation coverage and spring dust storms over northern China. *J. Geophys. Res.* **109**, D03104 (2004).
72. Shao, Y. *et al*. Dust cycle: An emerging core theme in Earth system science. *Aeolian Res.* **2**, 181–204 (2011).
73. Yu, J. *et al*. Geomorphic, hydroclimatic and hydrothermal controls on the formation of lithium brine deposits in the Qaidam Basin, northern Tibetan Plateau, China. *Ore Geol. Rev.* **50**, 171–183 (2013).
74. He, M., Zheng, J., Li, X. & Qian, Y. Environmental factors affecting vegetation composition in the Alxa Plateau, China. *J. Arid Environ.* **69**(3), 473–489 (2007).
75. Long, H. & Shen, J. Underestimated 14C-based chronology of late Pleistocene high lake-level events over the Tibetan Plateau and adjacent areas: Evidence from the Qaidam Basin and Tengger Desert. *Sci. China Earth Sci.* **58**(2), 183–194 (2015).
76. Yao, Z., Wang, T., Yang, J., Zhu, K. & Zhou, L. Analysis on frequently occurrence of dust storm in the Alxa Plateau. *J. Arid Land Resour. Environ.* **22**(9), 54–61 (2008).
77. Dong, Z. *et al*. Research progress in China's Lop Nur. *Earth-Sci. Rev.* **111**(1), 142–153 (2012).
78. Environmental and Ecological Science Data Center for West China (EESDCWC), National Natural Science Foundation of China, http://westdc.westgis.ac.cn. (2012).
79. Ma, J., Lv, C. & Wang, Q. Land-cover classification of the Qaidam Basin based on MODIS NDVI time series data. *Arid Land Geogr.* **31**(3), 442–448 (2008).
80. Wang, T., Yan, C. & Song, X. Remote sensing monitoring on land use changes of each ecosystem in Alax Prefecture of Inner Mongolia in last 30 years. *J. Desert Res.* **28**(6), 1001–1004 (2008).
81. Dou, Y., Chen, X. & Bao, A. M. Eco-environmental responses of land use and cover change in nearly 40 years in the Hetian River Basin. *Arid Land Geogr.* **31**(03), 449–455 (2008).
82. Li, Q. & Chen, X. Analysis on the landscape processing changes of Yarkant River Basin in recent 40 years. *J. Arid Land Resour. Environ.* **23**, 50–57 (2009).

83. Zhao, R. *et al.* Land use and land cover change and driving mechanism in the arid inland river basin: a case study of Tarim River, Xinjiang, China. *Environ. Earth Sci.* **68**(2), 591–604 (2013).
84. Zheng, X. Salt lakes on the Inner Mongolian Plateau of China. *Chin. Geogra. Sci.* **1**(1), 83–94 (1991).
85. Jin, C. *Highway construction and sand hazard controlling research in active dune region in the Taklamakan Desert.* Lanzhou: Lanzhou University (2006).

Acknowledgements

Author Contributions

X.W conceived and designed the experiments. W.M., L.J., L.L. and B.Z. collected samples. H.L., T.H. and D.L. completed wind tunnel experiments and particle size analysis; all authors analyzed the data; X.W. and H.C. co-wrote the paper. H.-Z.C., J.S., H.-Y.L. and M.Q. commented the manuscript.

Additional Information

Supplementary information accompanies this paper at doi:10.1038/s41598-017-09458-w

Competing Interests: The authors declare that they have no competing interests.

Publisher's note: Springer Nature remains neutral with regard to jurisdictional claims in published maps and institutional affiliations.